

EANDC (OR) - 115 "L"
2/72

EANDC (OR) - 115 "L"

INDC (SWD) - 4/L

Progress Report on Neutron Physics Research
in Sweden July 1972

The Research Institute of the Swedish
National Defence, Stockholm, Sweden

EANDC(OR)-115"L"

INDC(SWD)-4/G

Progress Report on Neutron Physics Research in Sweden July 1972

Compiled by

H. Condé and L.G. Strömberg

The Research Institute of the Swedish National Defence
Stockholm, Sweden

CONTENTS

Preface	1
Laboratories submitting contributions to this compilation	2
1. Neutron Physics	
1.1 Elastic and Inelastic Neutron Scattering	3
1.1.1 Measurements of fast neutron elastic scattering cross sections M.A. Etemad, B. Holmqvist and T. Wiedling Atomic Energy Company, Studsvik, Nyköping	3
1.1.2 On the search procedure in optical model calculations B. Holmqvist and T. Wiedling Atomic Energy Company, Studsvik, Nyköping	5
1.1.3 Optical model calculation of fast neutron elastic scattering cross sections for some reactor materials M.A. Etemad, B. Holmqvist and T. Wiedling Atomic Energy Company, Studsvik, Nyköping	8
1.1.4 Differential elastic neutron scattering cross sections in the energy interval 500 - 1400 keV S.G. Malmskog Atomic Energy Company, Studsvik, Nyköping	12
1.1.5 Gamma-rays from neutron induced reactions in nitrogen G. Nyström, H. Condé, B. Lundberg and L.G. Strömberg University of Lund and Research Institute of the Swedish National Defence, Stockholm	18

1.1.6	Gamma-rays produced by the interaction of 15 MeV neutrons in N, O, Mg and Al. K. Nyberg-Ponnert, B. Jönsson and I. Bergqvist University of Lund, Lund	19
1.1.7	The present status of fast neutron inelastic scattering measurements E. Almén, M.A. Etemad, B. Holmqvist and T. Wiedling Atomic Energy Company, Studsvik, Nyköping	20
1.1.8	Interpretations of the experimental fast neutron inelastic cross sections. E. Almén, B. Holmqvist and T. Wiedling Atomic Energy Company, Studsvik, Nyköping	22
1.2	Fission Physics	26
1.2.1	Studies of the fission threshold structure for ^{232}Th and ^{231}Pa M. Holmberg and L-E Persson The Research Institute of the Swedish National Defence, Stockholm	26
1.2.2	Prompt $\bar{\nu}$ -values of ^{235}U and ^{239}Pu in some fast reactor spectra. L. Widén and H. Condé The Research Institute of the Swedish National Defence, Stockholm	27
1.2.3	An experimental study of the prompt fission neutron spectrum induced by 0.5 MeV incident neutrons on ^{235}U P.I. Johansson, B. Holmqvist and T. Wiedling Atomic Energy Company, Studsvik, Nyköping	28

1.3	Neutron Capture	34
1.3.1	The (n, γ) cross section measuring facility J. McDonald Atomic Energy Company, Studsvik, Nyköping	34
1.3.2	Studies of fast neutron capture I. Bergqvist, B. Pålsson, B. Lundberg, A. Lindholm, L. Nilsson and J. Eriksson University of Lund, Lund, The Research Institute of the Swedish National Defence, Stockholm, Tandem Accelerator Laboratory, Uppsala, Atomic Energy Company, Studsvik, Nyköping	44
1.3.3	Measurements of gamma-rays and conversion electrons from (n_{th}, γ) reactions B. Fogelberg, A. Bäcklin and G. Hedin The Swedish Research Councils' Laboratory, Studsvik, Nyköping	46
1.3.4	Thermal neutron capture gamma-ray spectroscopy C. Larsson, L. Broman, J.P. Roalsvig, A.S. Alwash, E. Selin, L. Jonsson, S-O Berglund and H. Odelius Chalmers University of Technology, Gothenburg	47
2.	General Neutron Physics	52
2.1	Studies of $(d, p\gamma)$ reactions in nuclei with mass-numbers around $A = 50$ I. Bergqvist, L. Carlén and L. Nilsson University of Lund, Lund, Tandem Accelerator Laboratory, Uppsala	52

3.	Theoretical Physics	53
3.1	Shell model calculations of level densities	53
	J. Eriksson	
	Atomic Energy Company, Studsvik, Nyköping	
3.2	Calculation of semidirect nucleon radiative capture cross sections including spin-orbit and interference effects	55
	J. Eriksson	
	Atomic Energy Company, Studsvik, Nyköping	
4.	Van de Graff-accelerator, Studsvik	57
4.1	Accelerator performance	
	P. Tykesson and B. Jonsson	
	Atomic Energy Company, Studsvik, Nyköping	
4.2	Crossed field analyser	59
	P. Tykesson and B. Jonsson	
	Atomic Energy Company, Studsvik, Nyköping	
4.3	Installation of a solid state power supply	60
	P. Tykesson and B. Jonsson	
	Atomic Energy Company, Studsvik, Nyköping	
4.4	Change of accelerator tube	61
	P. Tykesson and B. Jonsson	
	Atomic Energy Company, Studsvik, Nyköping	
5.	Tandem Accelerator Laboratory, Uppsala	63
5.1	The neutron time-of-flight facility at the Uppsala Tandem Accelerator	63
	H. Condé, C. Nordborg, L-E Persson, L.G. Strömberg, A. Lindholm, G. Lodin and L. Nilsson	
	The Research Institute of the Swedish National Defence, Stockholm, University of Uppsala, Uppsala, Tandem Accelerator Laboratory, Uppsala	

Preface

This report gives information about neutron physics activities in progress at different laboratories in Sweden. This document contains information of a preliminary or private nature and should be used with discretion. Its contents may not be quoted, abstracted or transmitted to libraries without the explicit permission of the originator.

Laboratories submitting contributions to this
compilation

	Paragraph	Page
Neutron Physics Laboratory,	1.1.1, 1.1.2	3, 5
Atomic Energy Company, Studsvik,	1.1.3, 1.1.4	8, 12
Nyköping	1.1.7, 1.1.8	20, 22
	1.2.3, 1.3.1	28, 34
	1.3.2, 3.1	44, 53
	3.2, 4.1	55, 57
	4.2, 4.3	59, 60
	4.4	61
Department of Physics,	1.1.5, 1.1.6	18, 19
University of Lund, Lund	1.3.2, 2.1	44, 52
The Research Institute of the	1.1.5, 1.2.1	17, 26
Swedish National Defence,	1.2.2, 1.3.2	27, 44
Stockholm	5.1	63
Tandem Accelerator Laboratory,	1.3.2, 2.1	44, 52
Uppsala	5.1	63
The Swedish Research Councils'	1.3.3	46
Laboratory, Studsvik, Nyköping		
Chalmers University of	1.3.4	47
Technology, Gothenburg		
Department of Physics,	5.1	63
University of Uppsala, Uppsala		

1. Neutron Physics

1.1 Elastic and Inelastic Neutron Scattering

1.1.1 Measurements of fast neutron elastic scattering cross sections

M.A. Etemad, B. Holmqvist and T. Wiedling
Neutron Physics Laboratory, Studsvik, Nyköping,
Sweden

In previous fast neutron elastic scattering work performed at our laboratory angular distributions have been measured for 22 elements ranging from Al to Bi and in the energy range of 1.5 to 8 MeV. The experimental data have been used in a systematic investigation of the nuclear optical model. Five of the optical potential parameters, i.e. U , W , r_{OU} , r_{OW} and a have been varied with an automatic parameter search routine in order to get the best agreement between experimental and calculated angular distributions. The best fit parameters have been used to derive realistic generalized parameter values. The results of that investigation have recently been published [1]. Although the generalized parameters have been derived on the basis of more than 100 angular distributions there are still some gaps in certain mass and energy regions where the available experimental information is rather meager. It is for instance of particular interest to calculate scattering cross sections for fission products for which it is very difficult to collect experimental data with the present state of the art. The accuracy of such calculations increases with the amount of empirical data which is available for the derivation of the generalized potential. Therefore the measurements of fast neutron elastic scattering have been continued to fill some of these gaps. Up to now neutron

elastic scattering angular distributions have been measured at 7 MeV for the elements Mg, As, Nb, Mo, Cd, In, Sb, Hf, Au, Pb, radiogenic lead and Bi. The analyses of the data are in progress.

The shape of measured neutron elastic angular distributions are always distorted because of neutron attenuation and multiple scattering effects in the comparatively large scattering samples used. Corrections for these effects have been calculated with a Monte Carlo program [2]. The capability of this program has been tested by performing neutron scattering on cylindrical samples with the dimensions: height 50.0 mm, o.d. 25.0 mm and i.d. 9.5 mm and one with a height of 30.0 mm, o.d. 18.0 mm and i.d. 9.5 mm. The corrected differential neutron elastic scattering cross sections agree well within the accuracy of the measurements showing that the Monte Carlo code works satisfactory.

-
- [1] B. Holmqvist and T. Wiedling, Optical Model Analyses of Experimental Fast Neutron Elastic Scattering Data, AB Atomenergi, Studsvik, Sweden, Report AE-430 (1971).
- [2] B. Holmqvist, B. Gustavsson and T. Wiedling, A Monte Carlo Program for Calculation of Neutron Attenuation and Multiple Scattering Corrections, Arkiv Fysik 34 (1967) 481.

1.1.2 On the search procedure in optical model calculations

B. Holmqvist and T. Wiedling
Neutron Physics Laboratory, Studsvik, Nyköping,
Sweden

Nuclear scattering from atomic nuclei are frequently described in terms of the nuclear optical model. The commonly used local potential is characterized by a number of parameters defining the potential well of the interacting nucleon-nucleus system. This potential is of the analytical form

$$-V(r) = Uf(r) + iWg(r) + U_{SO} \left(\frac{\hbar}{\mu_{\pi} c} \right)^2 \frac{1}{r} \frac{d}{dr} |f(r)| \vec{\sigma} \cdot \vec{l}$$

with as many as seven parameters (U , r_{OU} , a , W , r_{OW} , b and U_{SO}). It has often been emphasized that the large number of parameters of the potential makes it unphysical to use with confidence since with as many as five to ten parameters it might be possible to describe almost any experimental data, and accordingly there would be no physical basis for the interpretation of the results. This is true, but usually it is possible to cancel most of the parameter sets on physical grounds. However, these circumstances make it difficult to apply the optical model potential with confidence. Hitherto the model has mainly been applied to scattered sets of experimental data with the resulting effect that it is difficult to draw accurate conclusions from comparisons of experiment with theory. Therefore, it is of great importance for systematic studies to collect a large set of experimental data with high accuracy for many elements in a large energy interval. A proper experimental data bank certainly gives the opportunity to test the optical model with confidence and reliability and to study its ambiguities.

The present investigation is concerned with some optical model calculations performed on the basis of angular distributions measurements of elastically scattered neutrons on a number of elements at 8 MeV. Details about the experimental data have been reported in previous publications [1, 2]. The calculations of angular distributions have been made with an automatic search program by varying five of the parameters, i.e. U , r_{OU} , a , W and r_{OW} . Treating b and U_{SO} as constants was not considered a serious draw-back, even if valuable information about the W - b coupling was lost. The influence of the spin-orbit term is rather small. The calculations have been performed three times for each element, the differences being mainly in the choice of the input value of r_{OU} which was 1.0, 1.2 and 1.3 fm, respectively. The low and high values are well below and above those usually accepted as normal.

The results of the parameter search calculations indicated some general features. Thus r_{OU} converged towards a value close to 1.2 fm, which is in agreement with the one normally accepted in previous investigations. However, a smaller value than 1.2 fm was found in those cases when $r_{OU}^{input} = 1.0$ fm. In about half of the cases studied this was compensated for by an increased value of U but in many of the remaining cases an unphysically low U -value resulted which indicated that a false minimum had been found. A better agreement between experimental and calculated elastic cross section data was obtained on the basis of $r_{OU}^{input} = 1.2$ and 1.3 fm than if a value of 1.1 fm was used. A conclusion which can be drawn from the results of the search procedures of optical model calculations is that the output data have to be carefully analysed if a reliable and accurate set of optical potential parameters are to be obtained.

An accurate analysis is also important from the point of view that a general description is obtained of experimental results from a range of nuclei and energies.

- [1] B. Holmqvist, Arkiv Fysik 38 (1968) 403.

- [2] B. Holmqvist and T. Wiedling, Optical Model Analyses of Experimental Fast Neutron Elastic Scattering Data, AB Atomenergi, Studsvik, Sweden, Report, AE-430 (1971).

1.1.3 Optical model calculation of fast neutron elastic scattering cross sections for some reactor materials

M.A. Etemad, B. Holmqvist and T. Wiedling
Neutron Physics Laboratory, Studsvik, Nyköping,
Sweden

Fast neutron elastic scattering cross sections are frequently requested for reactor core and shielding calculations [1]. However, there still exist both mass number and energy regions where there are no data, or very few data, available.

The aim of the present investigation was to obtain neutron elastic scattering cross section data for some elements frequently used as construction materials in reactors. The elements studied were Na, Al, Si, V, Cr, Mn, Fe, Co, Ni, Cu, Y, Nb and Pb and the energy range of interest was from 1.5 to 8.5 MeV. Some of these elements, i.e. Al, V, Cr, Mn, Fe, Co, Ni, Cu, Nb and Pb have been used in a previously reported [2] fast neutron elastic scattering study consisting of angular distribution measurements and interpretation of the data in terms of a spherical optical model potential. The parameters of this potential were used to derive a generalized optical potential. This potential has been used in the present work to calculate neutron elastic scattering cross sections and total cross sections for the elements and the energy range given above, in energy steps of 0.5 MeV. These calculations were carried out using the optical model program ABACUS-NEAREX and a CDC 6600 computer. The differential cross sections have been calculated in the centre of mass system at 21 angles for cosines between 1 and -1 in steps of 0.1. The cross sections calculated for the different elements have been compared with available

experimental data in order to check the validity of the generalized optical model potential in the mass and energy regions of the present work. This comparison is particularly interesting to do with the elements Na, Si and Y which were not used when deriving the potential parameters.

Since the experimental neutron elastic cross section is composed of a sum of the shape elastic cross section and the compound elastic cross section and it is only possible to calculate the former cross section with the optical model the latter one must be obtained by some other means. In this work the Hauser-Feshbach (H-F) method has been used to calculate the compound elastic contribution and its angular dependence. The most important limiting factor for these calculations is the lack of detailed information regarding the level properties of the target nucleus. For many nuclides there exist no data of this kind above 3 to 4 MeV. In many cases the level energies are given but the spins and/or parities are not known.

In those cases when the level energies were known but the spins and/or parities of a few levels were unknown the calculations were performed with estimated values for spins and/or parities. This has been found satisfactory since changing the value of the spin and parity of a few levels in the high-energy region will not affect the magnitude of the compound elastic cross section appreciably, at least when the number of levels are large, i.e. about 10 to 15.

Where no information about level properties is available above a certain energy, the values of the total compound elastic cross section at lower energies were

used to find the total compound elastic cross sections at higher energies by extrapolation. An exponential function of the form $A\exp(-BE)$ (E = energy in MeV) was chosen to fit the data at lower energies and to obtain the cross sections at higher energies. In those cases where the total compound elastic cross sections were found by extrapolation, the values of differential compound elastic cross sections were obtained simply by assuming the angular distribution to be isotropic. This method was believed accurate enough because it was applied only where several levels of the target nucleus were excited and accordingly the compound elastic contribution was rather small in comparison to the total elastic cross section, the former being less than about 15% of the latter cross section at 3.5 MeV and less than about 10% at higher energies for all elements studied in this work. Thus even an error of 30% in the estimated compound elastic cross section did not introduce an error in the calculated total cross section which was larger than the error in the corresponding measured cross section.

The results of the optical model and H-F calculations will be given in the form of tables which contain differential shape elastic, differential compound elastic and differential elastic cross sections as well as coefficients of Legendre Polynomials fitted to differential elastic cross sections. Also included in the tables are total (integrated) elastic cross sections, absorption (reaction) cross sections, nonelastic cross sections and total cross sections. These results will also be given on magnetic tape. The angular distributions will also be plotted and compared with the available experimental data. An example of an angular distribution is shown in Fig. 1.

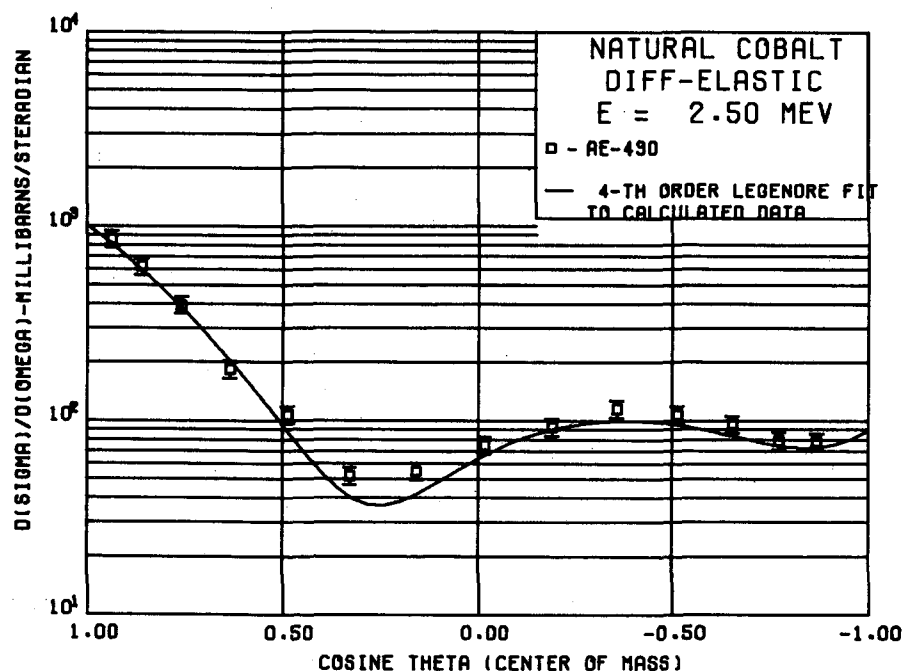


Fig. 1

Angular distribution of elastic scattering cross sections for Co. The solid line is the Legendre polynomial fit to calculated cross sections while points represent the experimental data of the given reference.

-
- [1] RENDA, Compilation of EANDC request for neutron data measurements. Compiled by W. Häusserman and S. Schwartz, ENEA/OECD, Paris 1968.
 - [2] B. Holmqvist and T. Wiedling, Optical Model Analyses of Experimental Fast Neutron Elastic Scattering Data, AB Atomenergi, Studsvik, Sweden, Report AE-430 (1971)

1.1.4 Differential elastic neutron scattering cross sections in the energy interval 500-1400 keV

S.G. Malmskog
Neutron Physics Laboratory, Studsvik, Nyköping,
Sweden

The conventional method of measuring differential elastic neutron scattering cross sections utilizes mono-energetic neutrons for bombarding the investigated sample and one detector, moved into different angles relative to the primary neutron beam, to detect the scattered neutron flux. To make an absolute measurement the scattered flux is compared to the scattered flux obtained by merely substituting for the first sample a standard sample with known scattering cross section, leaving all other experimental conditions as similar as possible. If the intentions are to determine the resulting angular distributions for many different bombarding neutron energies, the above-mentioned method requires hundreds of measurements, which make the experiment both time-consuming and expensive. Furthermore there are always difficulties in keeping the equipment stable enough to be able to accurately relate measurements made on different occasions over a period of several months, especially for cross section measurements in the resonance region.

At comparatively low neutron bombarding energies (below the first excited level of the sample nucleus) the only exit channel for neutrons is via the elastic scattering process. For such a process scattered neutrons at a certain angle for a definite energy can thus be unambiguously related to a definite primary neutron energy. This one-to-one relationship makes it possible to use several different neutron bombarding

energies at the same time and then separate the respective scattered neutrons using the characteristic scattered neutron energies. This can be done by using time-of-flight techniques, where the scattered neutrons will be separated in time according to their final energies and thus be registered in different channels in a final time-of-flight spectrum. In practice, however, it is very difficult to find suitable reactions to produce several separated neutron groups, and therefore one has to use reactions giving a continuous spectrum of primary neutrons.

The method sketched above has been used to determine the energy dependence of the differential elastic neutron scattering cross section for Cr, Fe, Ni, Al, Co and Y. The primary continuous neutron spectrum was obtained by bombarding a 1 mm thick, air-cooled Be target with 3.4 MeV protons at a mean current of 7 μ A. By studying the neutron elastic scattering in carbon it was established that the energy dependence of the neutron yield from the $^9\text{Be}(p,n)$ reaction was rather smooth and without prominent resonances. This primary neutron energy distribution, however, has a sharp high-energy side determined by the incident proton energy, which was chosen in such a way that the main part of the inelastically scattered neutrons would have an energy less than 500 keV. The reason for this energy limit is that, although the necessary energy discriminator to cut off the detector noise was set as low as possible, the neutron detector used (a 20 mm thick and 100 mm diameter NE104 plastic scintillator optically coupled to an RCA 8850 PM-tube) showed a useable neutron efficiency down to 200 keV. In the actual measurement on the carbon reference sample the background limited the useful lower scattered neutron energy detected to about 325 keV. At 150° this means a primary neutron energy of 450 keV, resulting in a

scattered energy of 425 keV using a Fe sample and measured at the same angle. Neutron spectra were recorded at the laboratory angles 30° , 40° , 60° , 80° , 100° , 120° and 150° . The total time resolution (FWHM) of the complete time-of-flight system as measured from the response function of mono-energetic neutrons from the T(p,n) reaction varied from 7 nsec (30 keV) at 500 keV to 3.5 nsec (35 keV) at 1400 keV. This measurement was also used for the energy and intensity calibration of the system.

For each angle one scattered neutron spectrum was registered for each of the elements Cr, Fe, Ni, Al, Co, Y and C (for reference) and a background measurement was made with the scattering sample removed but otherwise under identical conditions. The measured differential neutron scattering cross section $\sigma(\theta)$ can now be written

$$\sigma(\theta) \cdot A \cdot M = \sigma_C \cdot \left(\frac{N_C}{N}\right) \cdot \left(\frac{\epsilon_C}{\epsilon}\right) \cdot A_C \cdot M_C \cdot \left(\frac{C}{C_C}\right) \quad (1)$$

where the following notations have been used:

σ_C is the differential neutron scattering cross section for carbon used as a reference,

N and N_C are the numbers of atoms per cm^3 in each scattering sample,

ϵ and ϵ_C are the different efficiencies of the detector system at the scattered neutron energy for a constant primary neutron energy,

A and A_C are correction factors for neutron absorption in the scattering samples,

M and M_C take multiple scattering effects into account,

C and C_C are the total numbers of counts (corrected for background and normalized to a fixed number of primary neutrons) from a certain incident energy

interval ΔE and scattered through an angle θ . After scattering, this interval ΔE is transformed into a new interval ΔE_s , the magnitude of which depends on the mass number of the scattering sample and the scattering angle and is calculated from the kinematics of the elastic scattering process.

A computer program has been prepared which calculates the right-hand side of eq. (1) for any primary neutron group $E \pm \Delta E$. The value obtained is then used as a first approximation of the measured cross section, which is used as input to the computer program MULTSCAT 4 to make the final correction for neutron absorption and multiple scattering. Some examples of the resulting differential neutron scattering cross sections for Fe, Cr and Ni as a function of neutron energy for different scattering angles are shown in Fig. 1. Through integration the corresponding total cross sections are evaluated. An estimate of the errors in this latter cross section is given in Table 1. All the results obtained are available through the ENEA neutron data compilation centre and will also soon be published as AE-reports.

Table 1

Estimate of the errors in the measured total elastic neutron scattering cross sections.

Source of error	Error in %
Counting statistics (sample)	3
Counting statistics (reference)	3
Multiple scattering correction (sample)	3
Multiple scattering correction (reference)	2
Correction for neutron absorption (sample)	2
Correction for neutron absorption (reference)	2
Relative neutron detector efficiency	3
Total C(n,n) cross section	2
Total error	7%

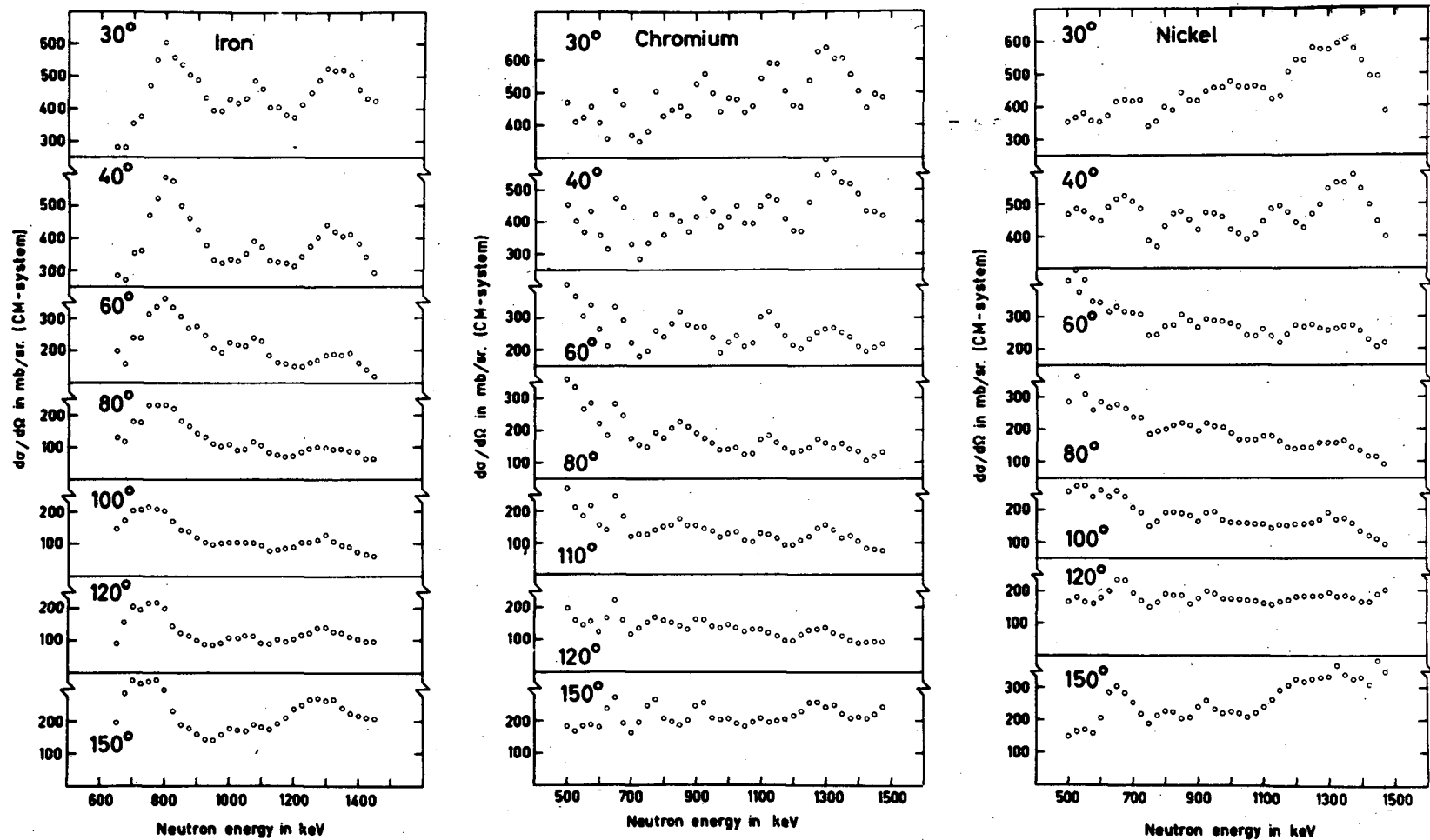


Fig. 1

The measured differential elastic neutron scattering cross section for the natural elements of Fe, Cr and Ni.

1.1.5 Gamma-rays from neutron induced reactions in nitrogen

G. Nyström^{x)}, H. Condé, B. Lundberg and
L.G. Strömberg
The Research Institute of the Swedish National
Defence, Stockholm, Sweden

The gamma-ray production cross sections of nitrogen have been measured at three different incident neutron energies, 4.2, 5.9 and 6.9 MeV at 55°. The gamma-ray spectrometer was a Ge(Li)-detector. Time-of-flight techniques were employed to suppress the background caused by neutron interactions in the Ge(Li)-detector. The efficiency of the gamma-ray spectrometer was measured with calibrated gamma-ray sources and (p,γ)-reactions. The primary neutron flux was measured with a proton-recoil telescope.

The angular distributions of the gamma-rays were measured at $E_n = 6.9$ MeV between 40° and 140°. The results were compared with calculated distributions obtained with a statistical compound-nucleus theory. The life-times of the six lowest excited states in ^{14}N could be estimated from the observed Doppler shifts in the angular distribution measurement.

The paper has been accepted for publication in *Physica Scripta* (1972).

x) University of Lund, Lund

1.1.6 Gamma-rays produced by the interaction of 15 MeV neutrons in N, O, Mg and Al

K. Nyberg-Ponnert, B. Jönsson and I. Bergqvist
Department of Physics, Lund University, Lund,
Sweden

Gamma-rays produced by 15 MeV neutron interactions in N, O, Mg and Al have been measured with a 7 mm Ge(Li) spectrometer. Differential γ -ray production cross sections at 80° have been determined relative to the cross section for the 4.44 MeV γ -ray line produced in $^{12}\text{C}(n,n')^{12}\text{C}$.

Physica Scripta (Sweden) 4, 165, 1971.

1.1.7 The present status of fast neutron inelastic scattering measurements

E. Almén, M.A. Etemad, B. Holmqvist and
T. Wiedling
Neutron Physics Laboratory, Studsvik, Nyköping,
Sweden

Fast neutron inelastic scattering cross sections have been measured over a period of three years at our laboratory. The purpose of this project has been to provide a relatively complete and homogeneous set of experimental inelastic scattering data for reactor core and shielding calculations. These data also give a good background for the proper understanding of the nuclear reaction mechanisms and of the usefulness of the nuclear models describing the scattering process. The experiments were performed with a time-of-flight spectrometer described in earlier reports from this laboratory.

Neutron inelastic scattering from the studied elements, i.e. Mg, Al, S, Ti, V, Cr, Mn, Fe, Co, Ni, Cu, Zn, Ga, Y, Nb, In, Pr, Ta, Pb, Pb_r (radiogenic lead) and Bi have been observed in the energy range of 2 to 4.5 MeV in steps of 0.25 MeV.

In order to determine the total neutron inelastic scattering cross sections for different levels of the elements studied, scattering was mostly observed at an angle of 125° , assuming the angular distributions to be isotropic or symmetric around 90° . The validity of this assumption has been investigated by observing differential inelastic scattering cross sections at several angles with an incident neutron energy of 3 MeV. Isotropy was observed in all cases except for the first excited states in ^{24}Mg and ^{32}S . For Mg the

the angular distributions were therefore also studied at 2.5, 3.5, 4.0 and 4.25 MeV incident neutron energies and for S at 3.5, 4.0 and 4.25 MeV.

Results for six of the elements, namely Al, V, Mn, Fe, Nb and Bi have already been reported [1]. Data analyses for another 8 elements, i.e. Mg, S, Ti, Ni, Cu, Y, Pb and Pb_r have been completed so far. The analyses of the data for the remaining elements are in progress.

-
- [1] E. Almén, M.A. Etemad, B. Holmqvist and T. Wiedling, Fast Neutron Inelastic Scattering in the Energy Range 2 to 4.5 MeV. Nuclear Data for Reactors (Proc. Conf. Helsinki, 1970) II, IAEA, Vienna (1970) 349.

1.1.8 Interpretations of the experimental fast neutron inelastic cross sections

E. Almén, B. Holmqvist and T. Wiedling
Neutron Physics Laboratory, Studsvik, Nyköping,
Sweden

Fast neutrons have proved to be a suitable tool for investigating the properties and structure of atomic nuclei. The purpose of this work is to provide a relatively complete and homogeneous set of experimental inelastic neutron scattering data. These data can give a good background for the proper understanding of the reaction mechanisms and of the usefulness of the nuclear models describing the scattering process. Such knowledge is of interest for reactor shielding calculations as well as from a pure nuclear physics point of view. Thus during the last three years fast neutron inelastic scattering from about twenty elements in the atomic mass region 24 to 209 has been measured with time-of-flight technique over an energy range of 2.0 to 4.5 MeV in steps of 0.25 MeV.

Since the inelastic scattering process is mainly characterized by compound nucleus formation in the investigated energy range, the interpretation of the experimental data was made in terms of the Hauser and Feshbach statistical model [1] corrected for level width fluctuations and resonance-interference effects using the computer program ABACUS-NEARREX.

According to Moldauer [2] the averaged compound nucleus cross section is then given by

$$\sigma_{nn'} = \pi \lambda^2 \sum_{\alpha\alpha'} g_{\alpha} \left\{ \left\langle \frac{\theta_{\mu\alpha} \theta_{\mu\alpha'}}{\theta_{\mu}} \right\rangle - M_{\alpha\alpha'} \right\}.$$

This expression consists of an average resonance term which is formally very reminiscent of the Hauser-Feshbach expression and of a resonance interference term

$$M_{\alpha\alpha'} = \frac{1}{4} \delta_{\alpha\alpha'} Q_{\alpha} \langle \theta_{\mu\alpha} \rangle^2.$$

In the absence of direct reactions the relation between the average over the resonance parameters $\theta_{\mu\alpha}$ (where μ denotes the resonance) and the optical-model transmission coefficient T_{α} is given by

$$\langle \theta_{\mu\alpha} \rangle = T_{\alpha} + Q_{\alpha}^{-1} [1 - (1 - Q_{\alpha} T_{\alpha})^{1/2}]^2.$$

The choice of the parameter Q_{α} is dependent on the properties of the compound nucleus. In the limit of infinitely many overlapping resonances the value of Q_{α} goes to zero while in the case of isolated resonances Q_{α} approaches one.

For the calculation of the transmission coefficients a knowledge of the proper nuclear potential is necessary. In this work a local optical potential including a spin-orbit interaction term has been used. The sets of parameters used in the calculations are taken from a recent investigation at our laboratory on generalized optical model parameters based on elastic scattering experimental data [3].

Comparisons of calculated cross sections with experimental data show that the pure Hauser-Feshbach model can overestimate the cross sections by as much as a factor of 2 at low primary energies where the statistical assumptions of the compound nucleus are not valid and only a few decay channels are available.

For most elements analysed so far good agreement with the experimental data is obtained taking the above mentioned corrections according to Moldauer into account and with the parameter Q_α set equal to zero, which as mentioned above indicates many overlapping levels in the compound nucleus. As an example Fig. 1 shows the experimental and theoretical excitation functions for V and Fe.

-
- [1] W. Hauser and H. Feshbach, Phys.Rev. 87 (1952) 366
 - [2] P.A. Moldauer, Phys.Rev. 135B (1964) 642
 - [3] B. Holmqvist and T. Wiedling, Optical Model Analyses of Experimental Fast Neutron Elastic Scattering Data, AB Atomenergi, Studsvik, Sweden, Report, AE-430 (1971)

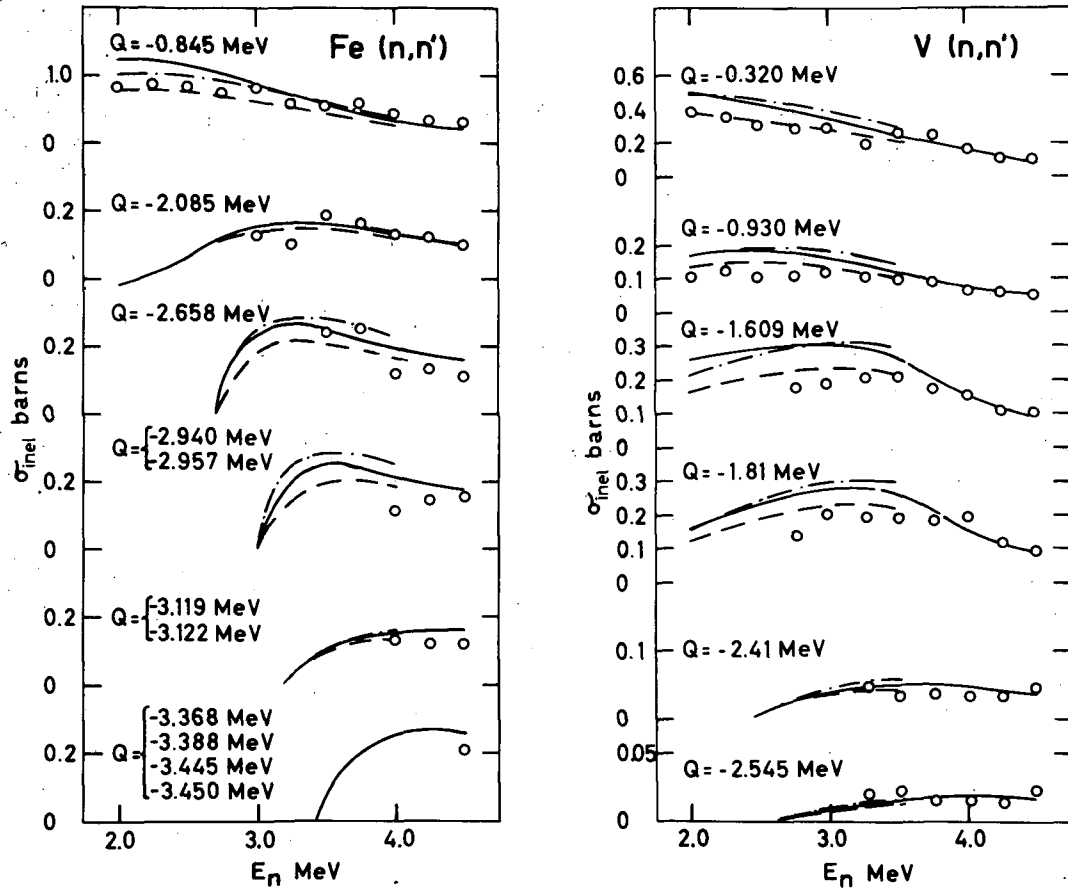


Fig. 1

Excitation functions for inelastic scattering from V and Fe. The experimental results (circles) are compared with cross sections calculated by use of the Hauser-Feshbach formalism (solid lines) as well as with cross sections calculated according to Moldauer with $Q_\alpha = 0$ (dashed lines) and $Q_\alpha = 1$ (the third line).

1.2 Fission Physics

1.2.1 Studies of the fission threshold structure for ^{232}Th and ^{231}Pa

M. Holmberg and L-E Persson
The Research Institute of the Swedish National,
Defence, Stockholm, Sweden

Measurements of the fission cross section and of the angular distributions of the fission fragments have been made for ^{232}Th and ^{231}Pa . The "Makrofol" technique is used in the measurements of the angular distributions. The results have been analyzed and are prepared to be published.

1.2.2 Prompt $\bar{\nu}$ -values of ^{235}U and ^{239}Pu in some fast reactor spectra

L. Widén and H. Condé
The Research Institute of the Swedish National
Defence, Stockholm, Sweden

The averaged number of prompt neutrons per ^{235}U and ^{239}Pu fission have been measured in fast and thermalized neutron fluxes at the fast zero-power reactor (FRO) at Studsvik, Sweden. The measurements were made with three different reactor cores giving median neutron energies of 50, 170 and 240 keV. The spectrum averaged $\bar{\nu}$ data were compared with the corresponding thermal $\bar{\nu}$ data. The fission samples were placed in neutron beams extracted from the reactor cores and a large liquid scintillator was used as the fission neutron detector. The experiment also included relative fission rates measurements, $^{238}\text{U}/^{235}\text{U}$, for the three reactor cores.

The results were compared with calculated $\bar{\nu}$ -values deduced from different sets of recently evaluated fission cross section and $\bar{\nu}$ -data and from different assumptions concerning the reactor neutron spectra. Within the experimental errors of about 1.5% a good agreement was obtained assuming $\bar{\nu}$ -values in the fission resonance region equal to $\bar{\nu}$ at thermal energy.

1.2.3 An experimental study of the prompt fission neutron spectrum induced by 0.5 MeV incident neutrons on ^{235}U

P.I. Johansson, B. Holmqvist and T. Wiedling
Neutron Physics Laboratory, Studsvik, Nyköping,
Sweden

The shapes of prompt fission neutron spectra of the main fissile and fertile isotopes have recently attracted great interest, although previously it had been assumed that these spectra had been measured with satisfactory precision. Despite the many microscopic measurements made of prompt fission neutron spectra the results of different experimenters disagree by amounts exceeding the given error uncertainty indicating the existence of large systematic errors. Furthermore, the macroscopic measurements recently performed indicated appreciably harder spectra than those extracted from microscopic measurements. The general shapes of the spectra are known, but accurate relative intensities are not well known above 7 MeV and below 2 MeV where the microscopic and macroscopic measurements differ most. One possible reason for the discrepancies between fission spectra observed at different laboratories by using a scintillator detector may be uncertainties in the measurements of the detector efficiency curve. The methods of calculating this curve of the use of angular distributions of neutron source reactions, i.e. $\text{T}(\text{p},\text{n})^3\text{He}$, $\text{D}(\text{d},\text{n})^3\text{He}$, etc. to measure the response function do not give sufficient precision. A more accurate way which has been used in the present experiment is to measure the efficiency curve by observing angular distributions of the well known n-p scattering process at different energies.

This investigation is concerned with the fission neutron spectrum from ^{235}U using time-of-flight techniques at an incident neutron energy of 0.53 MeV. The purpose was to measure the fission spectrum over as large an energy range as possible, i.e. from 0.6 MeV to 15 MeV. A comparatively large liquid scintillator was chosen as a detector element in order to get a high efficiency extending over a large energy range, good time resolution and the possibility of using pulse shape discrimination to suppress the gamma background. This experimental technique has given very positive results in that it has enabled the recording of a fission neutron spectrum with very satisfactory statistics from about 0.5 MeV up to the highest fission neutron energy. The background conditions were extremely good even up in the high-energy range, thus giving an extraordinary accuracy for an experiment of this type. The detector arrangements were located in a large shielding of lithium paraffin, iron and lead. The distance between the uranium sample and the detector was 300 cm at a detector angle of 90° relative to the incident neutron beam. Neutrons of 0.53 MeV energy were produced by the $^7\text{Li}(p,n)^7\text{Be}$ reaction and the relative neutron flux was monitored with a direction-sensitive long counter.

It is very important in measurements of this type, requiring accurate determinations of intensities in different energy intervals covering a large energy range, that the energy scale as well as the energy dependence of the neutron detector be known with high accuracy. The energy calibration of the time-to-pulse-height converter of the neutron spectrometer was performed by observing neutron groups from the reactions $\text{T}(p,n)^3\text{He}$, $^9\text{Be}(d,n)^{10}\text{B}$ and $\text{T}(d,n)^4\text{He}$ as well

as neutron scattering from hydrogen and carbon. The energy covered was 0.5 MeV to 21 MeV.

The relative efficiency of the neutron detector was determined as mentioned by observing neutron scattering from hydrogen at different primary energies and at different angles. For these measurements new target facilities have been used allowing the production of high neutron flux intensities. This equipment in combination with the pulse shape discrimination made it possible to measure the detector response function with high accuracy from 0.9 MeV to 15 MeV with the n-p scattering process. The low-energy part of the efficiency curve has been measured by detecting neutrons from the $T(p,n)^3\text{He}$ reaction. Thus the energy range from 0.5 to 15 MeV was covered. In this experiment requiring long running time the efficiency curve as well as the time calibration of the spectrometer was performed before as well as after the fission experiment.

At fast primary neutron energies the analysis of fission neutron spectra recorded by time-of-flight techniques become somewhat complicated because of the interference between the continuous fission spectrum and neutrons emitted in competing elastic and inelastic scattering processes. The high-energy end of the fission spectrum may also be somewhat influenced by the low-energy tail of the peak from sample gammas incident on the detector. The distortion of the high-energy region of the neutron spectrum by the gamma peak has been drastically diminished by pulse shape discrimination. The contributions to the fission spectrum caused by the high-energy tail of the elastic peak were taken care of by subtracting neutron scattering spectra recorded with a ^{181}Ta sample.

The corrections for flux attenuation in the uranium sample have been performed on the basis of Monte Carlo technique. The relative correction factor was found to vary little with the fission neutron energy, i.e. between 1.03 and 0.99. Up to now the effects of neutron multiple scattering on the shape of the fission neutron spectrum have been considered to be small and have accordingly been neglected. However, a more careful investigation of the importance of the multiple scattering effects is highly desirable.

The standard procedure to interpret the fission neutron spectrum from microscopic measurements has been to fit a semi-empirical function derived from nuclear evaporation theory to the experimental data. A function chosen is the one proposed by Watt:

$$N_W(E) = k_1 \exp(-E/A) \sinh(BE)^{\frac{1}{2}}$$

Here E is the neutron energy, k_1 is a normalization factor and A and B are constants chosen to fit the data points. Another function used is the Maxwellian distribution proposed by Terrell:

$$N_M(E) = k_2 E^{\frac{1}{2}} \exp(-E/T)$$

Here E is the neutron energy, k_2 is a normalization constant and T is the so called Maxwellian temperature. Since there is no theoretical reason for using one or the other form, the Maxwellian distribution has hitherto been most commonly used.

Experimental data are shown in Fig. 1 as the number of fission neutrons per unit energy interval, $N(E)_{\text{exp}}$, divided by $E^{\frac{1}{2}}$ with arbitrary normalization. It is shown that the Watt distribution (dotted line) fits

the data over the entire energy range. The best fit parameters are $A = (1.01 \pm 0.03) \text{ MeV}$ and $B = (2.34 \pm 0.30) \text{ MeV}^{-1}$. The least-squares fit with the Maxwellian distribution (solid line) gave the parameter: $T = (1.42 \pm 0.01) \text{ MeV}$. It is evident that the Maxwellian distribution does not fit the data points as well as is possible with Watt's distribution.

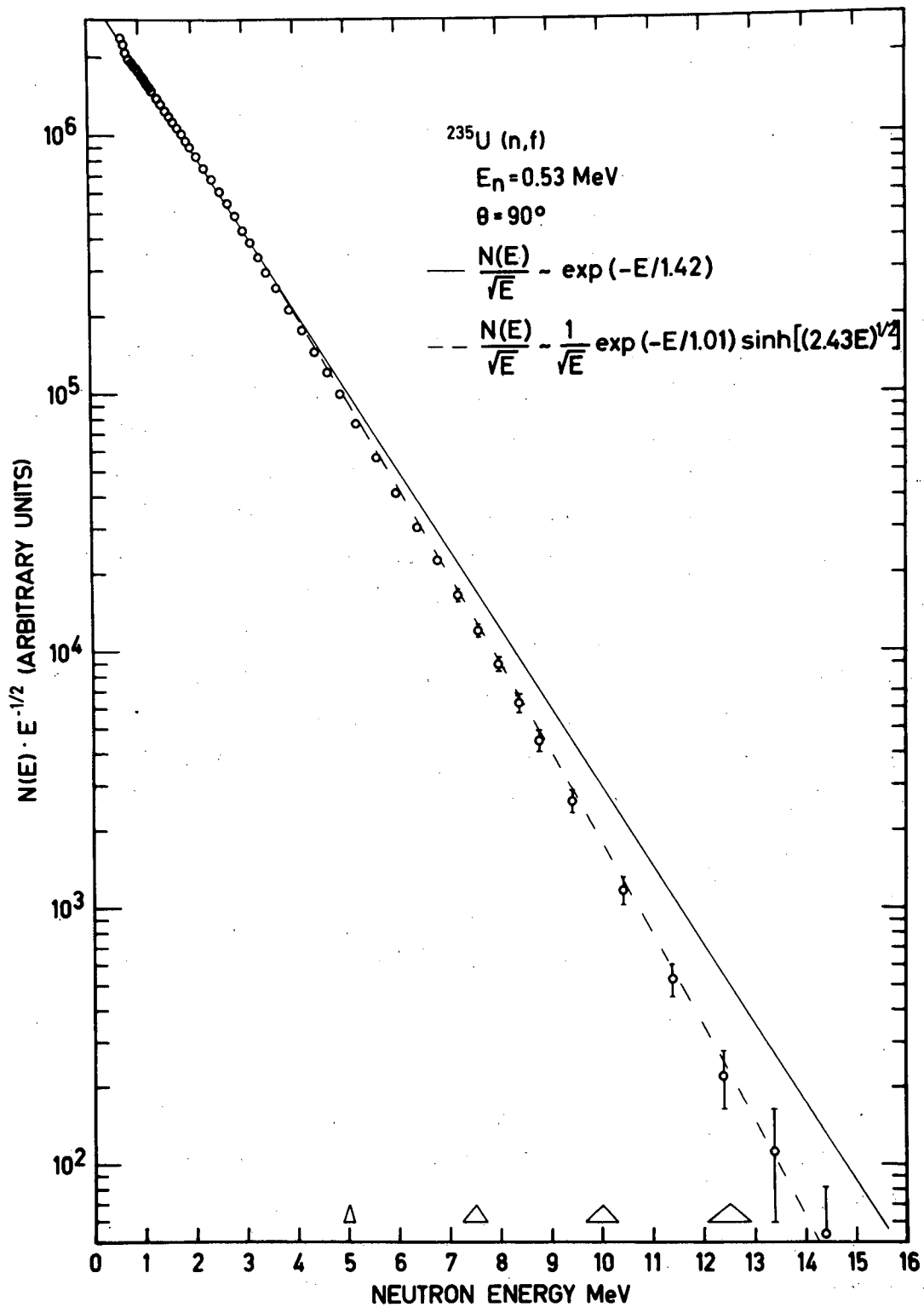


Fig. 1

The fission neutron spectrum from ^{235}U obtained at 0.53 MeV incident neutron energy. The solid line and the dotted line are least squares fits to the experimental points assuming Maxwellian distribution and Watt distribution respectively.

1.3 Neutron Capture

1.3.1 The (n, γ) cross-section measuring facility

J. McDonald

Neutron Physics Laboratory, Studsvik, Nyköping,
Sweden

For the measurement of (n, γ) cross-sections at the 6MV Van de Graaff at Studsvik a cylindrical tank containing 200 l of NE218 liquid scintillator is used to detect the prompt γ -rays following neutron capture in a sample placed in the centre of the tank, which is optically divided into two halves. The fast pulsed beam from the accelerator produces neutrons in a ^7Li target. Samples are investigated by measurements relative to suitable standard materials, in the present case Au and In for which adopted values for capture cross-sections in the energy range 10 keV to 10 MeV have recently been tabulated [1].

It can be shown that

$$\frac{\sigma_x}{\sigma_{\text{std}}} \propto \frac{A_x}{A_{\text{std}}} \cdot \frac{f_{\text{std}}}{f_x}$$

where:

σ_x and σ_{std} are the capture cross-sections of the sample and the standard material at the selected neutron energy;

A_x and A_{std} are the respective areas of the peaks in the time spectra due to the neutron capture;

f_x and f_{std} are the fraction of the detected capture γ -ray pulses which are accepted by the energy single channel analyser.

Hitherto the majority of γ -detectors used have been large volume liquid scintillators, which ideally should

be 100% efficient for the detection of the prompt γ -radiation which follows neutron capture. For such an ideal detector each capture event should give a pulse corresponding to the neutron binding energy plus incident energy (usually ≈ 8 MeV). In practice the pulse heights are smeared out by the scintillator resolution and by partial escape of radiation, which results in a significant low energy component in the detector response. This component cannot be separated from the high background which is unavoidable with such detectors, and which must be discriminated against by setting an energy threshold. It is this energy selection which introduces the factors f in equation (a), and which necessitates careful study of the sample energy spectra. In most neutron capture events the nucleus de-excites by emitting a cascade of γ -rays so that by demanding a fast coincidence between each half of the divided detector such events are preferentially selected and background correspondingly reduced. (For energies above 1 MeV the γ -ray background was reduced by a factor of 20, and above 2.2 MeV by a factor of 10). A further important benefit of this system is that the energy signal from the tank must be composed of the sum of at least two gamma interactions, so that the centroid of the spectrum is shifted to higher energies. In this way the detector can be said to behave more like a tank of larger volume without the corresponding background difficulties.

This feature is also helpful for accurate determination of the spectrum fraction factors f in equation (a) which are important and sensitive quantities for these measurements. There is one possible disadvantage of the split-tank feature and this is being investigated. In certain nuclei a non-negligible fraction of decays

proceed by a low-multiplicity cascade, containing a high energy γ -transition, with a corresponding chance of escape from the detector. This is thought to be the case for fast neutron capture in Au [2], which is particularly serious for comparison measurements in which Au is used as the standard, and can be a possible source of systematic error. Since In is known to have a high gamma multiplicity as well as a higher absolute cross-section than Au for neutron energies above 20 keV it is a better choice as a standard sample for comparison measurements with this apparatus. It is clearly of considerable importance to study the pulse height spectra obtained for different samples and different neutron energies. With the split tank arrangement this response is particularly sensitive to the selection conditions used in the electronics, but the new system shown in Fig. 1 has proved to give excellent performance. Several new features have been incorporated in order to handle high count rates and to reduce measuring times. These are described in detail in an internal report (FN-TPM-20, 1972). The measurement of energy spectra and hence the f factors will be further simplified when the PDP-15 computer is used for on-line data collection and handling. This system will be incorporated for the next series of experiments.

Preliminary measurements have been made with an Ag sample at a neutron energy of 200 keV. (All samples are discs 11 cm in diameter and 1 mm thick). Comparison samples of In and Au were used. Time-of-flight spectra obtained with the Ag sample are shown in Figs. 2a and 2b. The relevant gamma energy spectra are given in Fig. 3 together with the two energy threshold settings used. The data of Fig. 2a were taken with the high

threshold setting, and a signal to background ratio of 1.6 was obtained for the sample peak. The counting rate in the peak was 12 per second. From Fig. 4 it can be seen that the high threshold position corresponds to an f factor of 0.31 for Ag. The time-of-flight spectrum of Fig. 2b was taken with the low threshold setting. Despite the large number of background gamma rays accepted (evident from Fig. 3) the sample peak had a signal to background of 0.5, while the peak count rate increased to 28 per sec. From Fig. 4 the corresponding f factor is 0.75. (The same neutron flux was used for all measurements). The Ag data were compared with In measurements for both low and high threshold settings, and taking the adopted value [1] of 254 mb for σ_{In} at $E_n = 200$ keV cross sections of 270 and 264 mb respectively were derived for σ_{Ag} . This agreement is encouraging in view of the very different experimental conditions, and gives confidence in the reliability of the method and in the f factor determinations. However, when the low threshold data were compared to those obtained with an Au sample (for which a value of $\sigma_{\text{Au}} = 260$ mb was taken [1]) a value of $\sigma_{\text{Ag}} = 380$ mb was obtained. There is thus a difference of over 40% between the Ag cross-sections derived from comparison studies with the two different standard samples. (It should be noted that the cross-section values quoted are preliminary and have not been corrected for multiple scattering or self-shielding. However, such corrections will be <10% and cannot account for the observed difference. For these reasons no error estimation has been quoted for σ_{Ag}).

The higher value obtained using the Au comparison sample can be explained from the harder Au capture γ -ray spectrum 2 which will result in the loss of a significant number of events from the split tank. This effect should be present to a lesser degree with conventional large scintillator tanks, and may help to explain the large spread (from about 250 - 500 mb) in the tabulated experimental values [1, 3] for σ_{Ag} at ≈ 200 keV neutron energy.

There is in fact a systematic difference in published values [3] of the (n, γ) cross sections for Ag for neutron energies above 60 keV, and it is intended to make comparison measurements with the In and Au standard samples over a large range of neutron energies in order to determine to what extent the effects discussed above contribute to this difference. Measurements will also be made with a Cd sample, since the presently available data show a considerable divergence from the theoretical estimates of Benzi et al [1].

Finally it is intended to study samples of Ni, Fe and Cr for which (n, γ) cross sections in the keV to MeV range are urgently needed for reactor calculations [4].

[1] V. Benzi et al., CNEN report Doc. CEC (71) 9

[2] B.C. Diven et al., Phys. Rev. 120 (1960) 556

[3] A.D. Carlson, Gulf-RT-10387 (1970)

[4] H. Häggblom, AE report, to be published (1972)

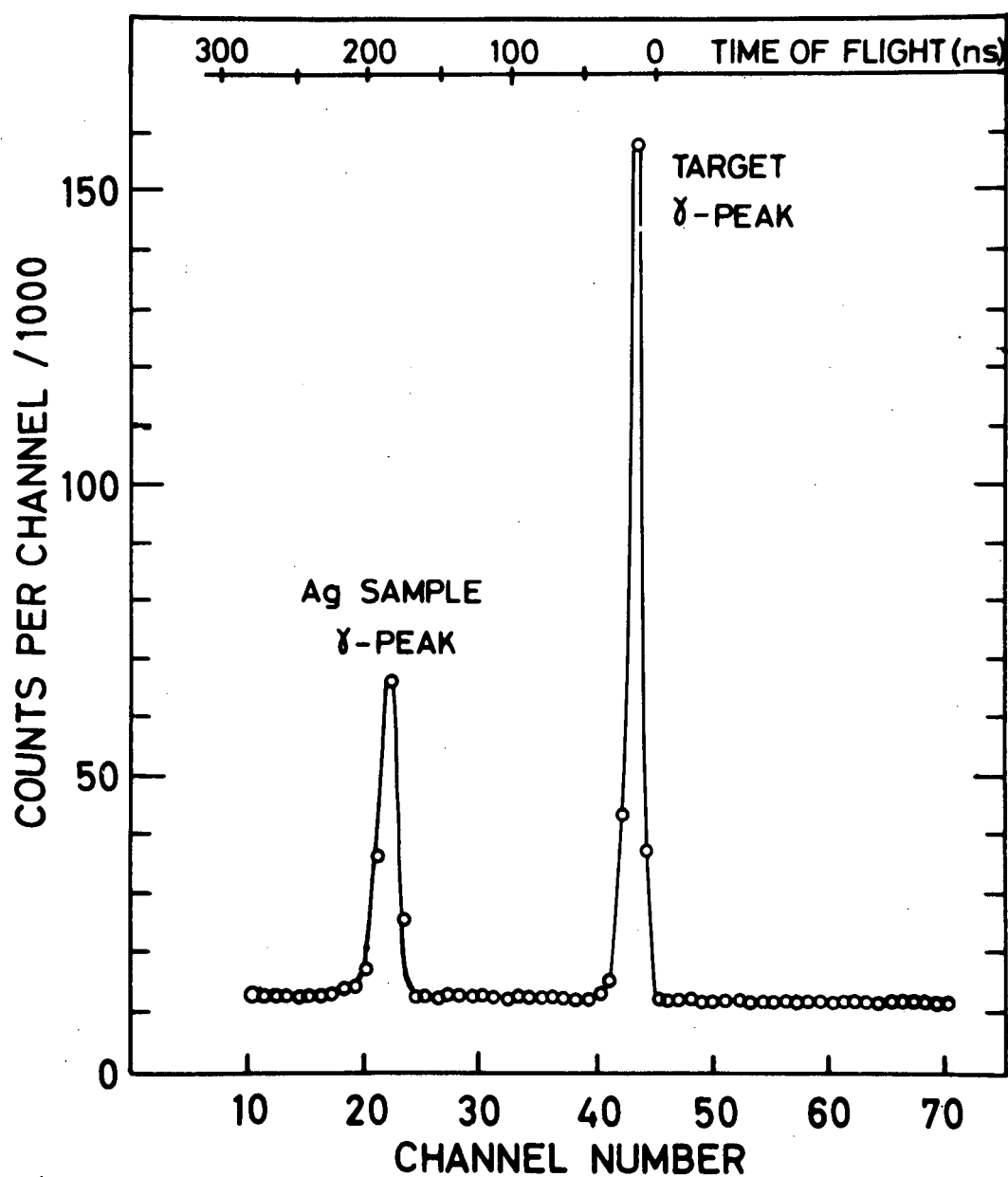


Fig. 2a

Time-of-flight spectrum for Ag at a neutron bombarding energy of 200 keV. A thin Li target was used. The energy selector was set to the high threshold position (see Fig. 3).

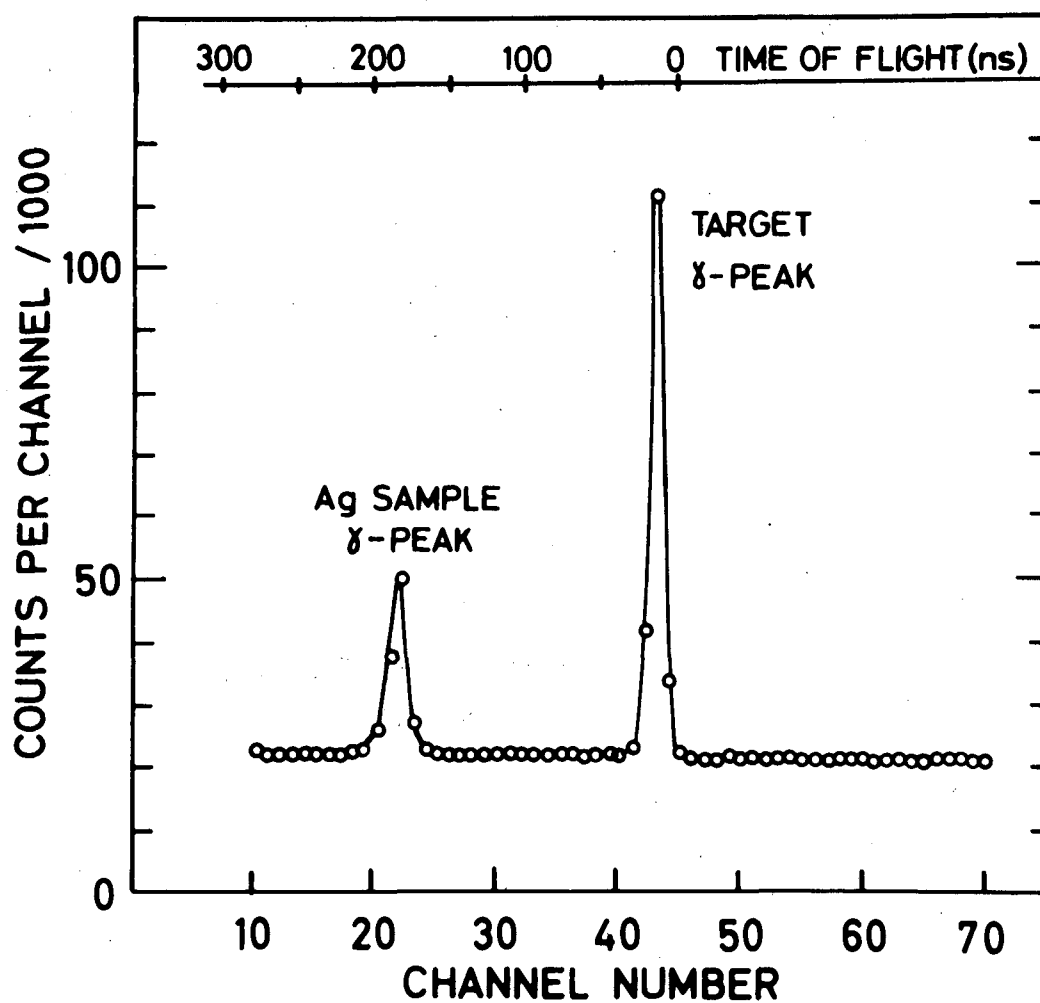


Fig. 2b

Similar to spectrum of Fig. 2a. The energy selection was set to the low threshold position (see Fig. 3).

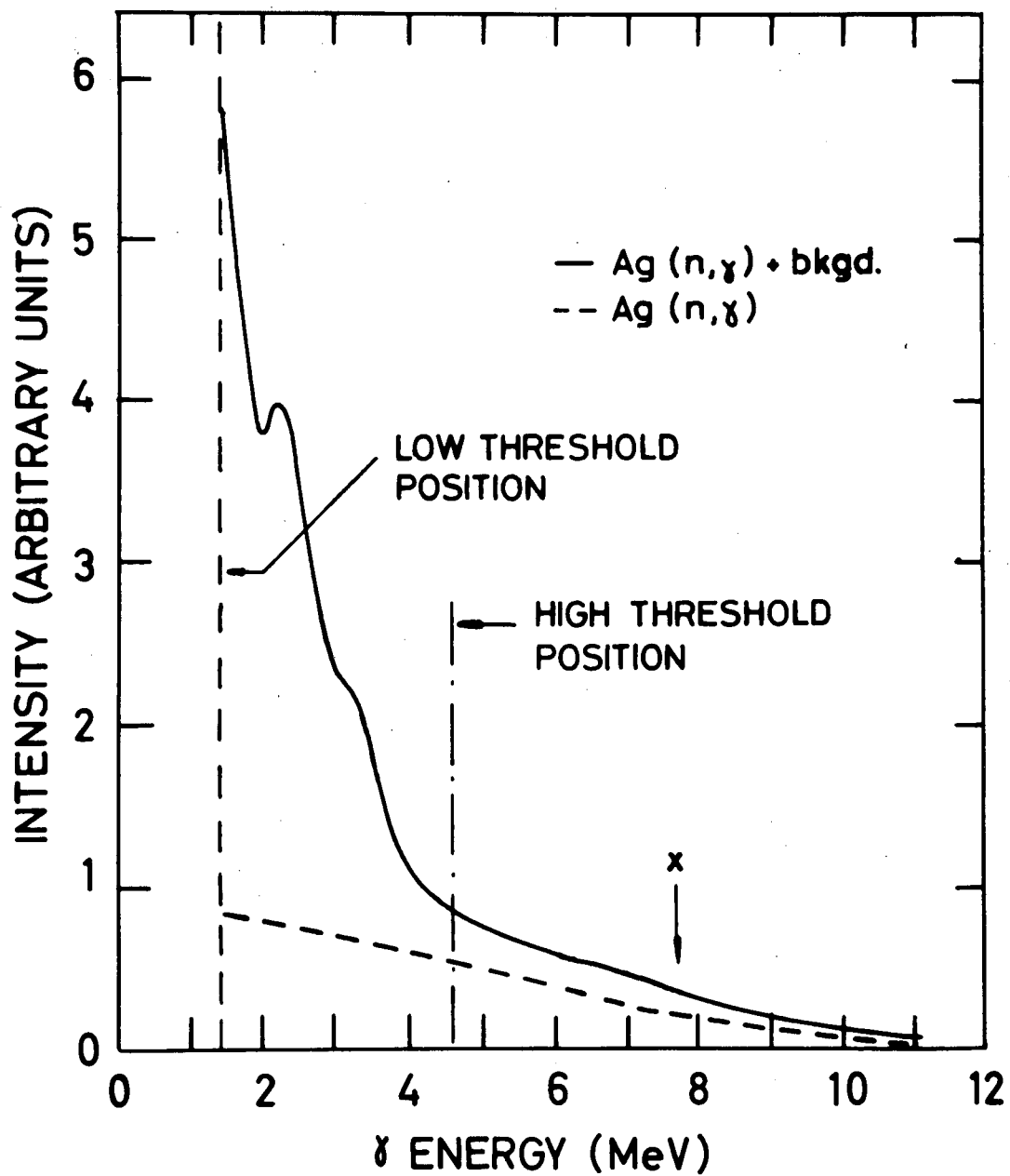


Fig. 3

Gamma ray spectra with and without background subtraction obtained from the tank using a Ag sample and 200 keV neutrons. Energy threshold positions are indicated, as well as the approximate total γ -ray energy (Indicated by 'X').

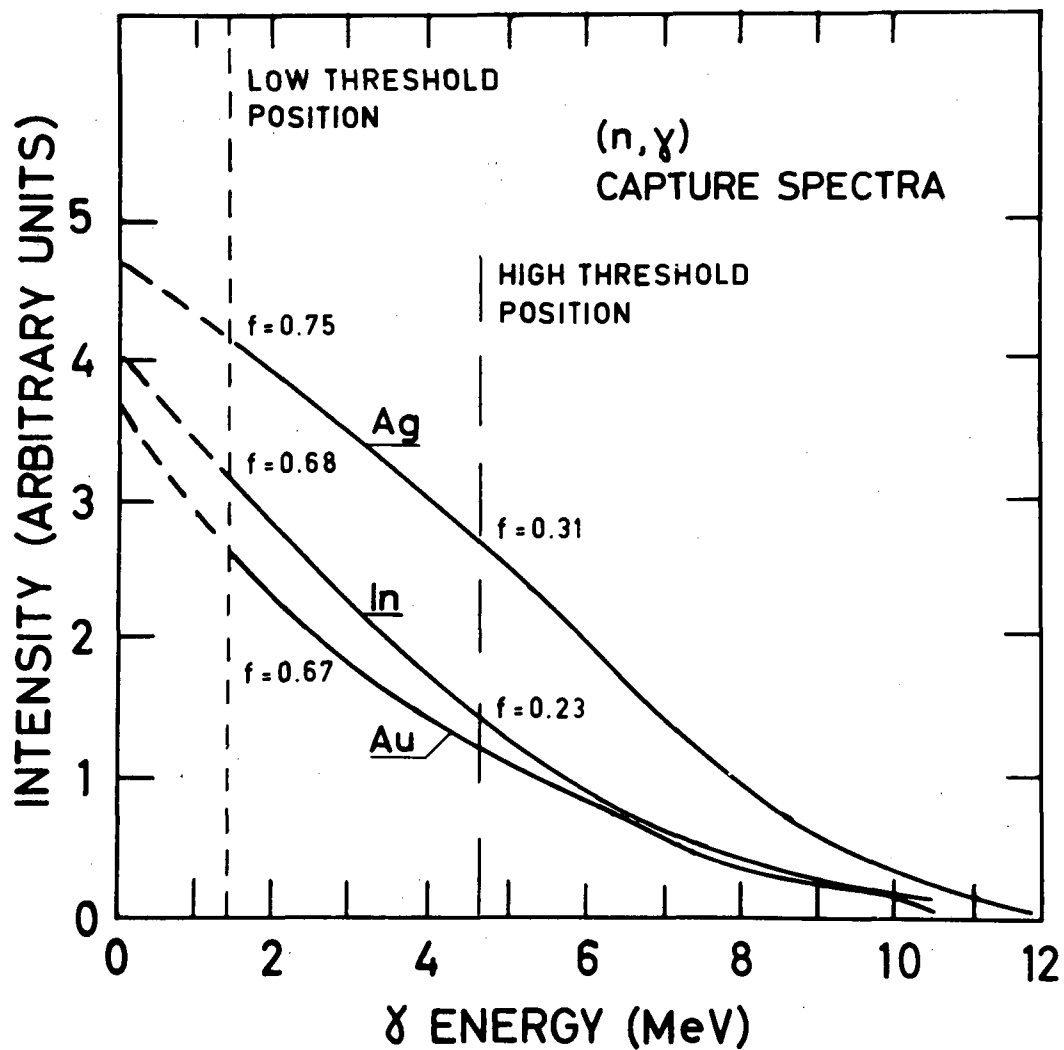


Fig. 4

Energy spectra for 200 keV neutrons incident on samples of Ag, In and Au. Background has been subtracted. High and low threshold positions are indicated, as well as the relevant f-factors derived from the shapes of the spectra. (The shapes below 1.3 MeV were obtained by extrapolation).

1.3.2 Studies of fast neutron capture

I. Bergqvist and B. Pålsson
 Department of Physics, University of Lund, Lund
 B. Lundberg ^{x)}
 The Research Institute of the Swedish National
 Defence, Stockholm, Sweden

A. Lindholm and L. Nilsson
 Tandem Accelerator Laboratory, Uppsala, Sweden

J. Eriksson
 AB Atomenergi, Studsvik, Nyköping, Sweden

Measurements of (n, γ) reaction cross sections in the giant dipole resonance region have for several years been performed at the 5.5 MeV van de Graaff accelerator at Studsvik. Neutrons of energies below 8.5 MeV were produced by the $^2\text{H}(d, n)^3\text{He}$ reaction. This energy limitation implies that in most nuclei it is not possible to reach the peak of the giant dipole resonance. At the tandem accelerator in Uppsala monoenergetic neutrons of energies up to 11 MeV can be produced by the $^3\text{H}(p, n)^3\text{He}$ reaction, which means that the peak of the giant dipole resonance in many nuclei can be covered.

Earlier work [1,2] has shown that the semi-direct reaction model reasonably well accounts for capture cross sections in the giant dipole resonance region for nuclei with neutron numbers around $N = 28$ (^{58}Ni and ^{60}Ni), whereas for nuclei with $N \approx 126$ (^{206}Pb and Bi) the model predicts cross sections 2 - 3 times smaller than the experimental ones.

The experimental work has been extended in two directions. The measurements now include a number of nuclei in a wide mass range i.e. Si, S, Y, I and Ce. Cross section measurements with 15 MeV neutrons have also

x) Present address: The Swedish Institute for the Handicapped, Stockholm

been initialized using the $^3\text{H}(d,n)^4\text{He}$ -reaction for neutron production. A further extension of the neutron energy range to include 8 - 11 MeV will be done after the transfer of the detector and target equipment to the Uppsala tandem accelerator. Measurements in this energy range are planned for the beginning of the autumn.

The computer code written to calculate cross sections has been modified to include both direct capture and interference between direct and semi-direct capture. Some effort has also been spent to investigate the influence of different parameter choices on the calculated cross section. These calculations [3] has primarily been performed for the $^{208}\text{Pb}(n,\gamma)$ reaction in connection with experiments performed at Los Alamos [4].

The data reduction for Si and S is being completed and preliminary results will be given this summer at the Budapest Conference on Nuclear Structure Study with Neutrons. Analysis of data on Y, I and Ce is being performed.

-
- [1] I. Bergqvist et al., Nucl. Phys. A 120 (1968) 161
 - [2] I. Bergqvist et al., Nucl. Phys. A 153 (1970) 553
 - [3] J. Eriksson and L. Nilsson, to be published
 - [4] I. Bergqvist et al., Phys. Rev., to be published

1.3.3 Measurements of gamma-rays and conversion
electrons from (n_{th}, γ) reactions

B. Fogelberg, A. Bäcklin and G. Hedin
The Swedish Research Councils' Laboratory,
Studsvik, Nyköping, Sweden

No experiments have been performed due to a waterleak in the neutron channel from the reactor core. The analysis of previously obtained data have resulted in manuscripts on the level structures of ^{156}Gd and ^{236}U .

1.3.4 Thermal neutron capture gamma-ray spectroscopy

Chalmers University of Technology, Gothenburg
Sweden

a) Level structure of ^{36}Cl

C. Larsson, L. Broman, J.P. Roalsvig, A.S. Alwash

The results of earlier measurements have now been treated. The combined diffraction crystal and Ge(Li) spectrometer has made it possible to measure 50 transitions in ^{36}Cl in the region 500 to 2600 keV, in which it has the most favourable peak to background ratio. Half of these transitions were previously not reported. Most lines could be fitted into a decay scheme extended by 5 new levels in addition to the earlier known ones. The existence of the new levels is further established by combinations between them and the capturing state. The results have been prepared for publication.

b) Level structures of ^{164}Dy and ^{165}Dy

C. Larsson, J.P. Roalsvig, M. Alwash, E. Selin

The data collection from the reactions $^{163}\text{Dy}(n,\gamma)^{164}\text{Dy}$ and $^{164}\text{Dy}(n,\gamma)^{165}\text{Dy}$ using enriched dysprosium isotopes has been concluded and the results prepared for publication.

c) Level structures of ^{51}Cr , ^{53}Cr and ^{54}Cr

C. Larsson, L. Jonsson, S.-O. Berglund, H. Odelius

The earlier started studies of the reactions $^{50}\text{Cr}(n,\gamma)^{51}\text{Cr}$, $^{52}\text{Cr}(n,\gamma)^{53}\text{Cr}$ and $^{53}\text{Cr}(n,\gamma)^{54}\text{Cr}$ using enriched isotopes have been continued. The analyses of the spectra are in progress.

d) Development of a method for measuring of the protein contents in seeds

C. Larsson, P.N. Tiwari

This work has been performed in collaboration with Dr. A. Bäcklin. In order to increase the protein contents in seeds by breeding it is necessary to know a non-destructive method for measuring the protein contents. Assuming a close relation between the protein and the nitrogen contents, the problem is reduced to development of a non-destructive method for measuring the nitrogen contents. It has been proposed (Tiwari) to use the $^{14}\text{N}(n,\gamma)^{15}\text{N}$ -reaction for that purpose.

Preliminary experiments have been performed using a thermal neutron beam with a flux of $4 \cdot 10^5$ neutrons/cm² · sec obtained by double diffraction in copper crystals of a neutron beam from the R2 reactor. The flux of fast neutrons was <10 neutrons/cm² · sec and the gamma-ray flux of the order of 1 m rem/h. The 10.8 MeV gamma line from the $^{14}\text{N}(n,\gamma)^{15}\text{N}$ -reaction, the intensity of which amounts to 14% per capture, was recorded with a 3" x 3" NaJ detector shielded by 15 cm of lead to reduce the background. In front of the detector a 7 mm thick lead absorber was inserted in order to reduce the counting-ratio at low energies. The samples were surrounded by a rod made of 5 mm thick boron-plastic, in order to decrease the (n,γ) radiation from the lead shield caused by the neutrons scattered from the samples.

Fig. 1 shows spectra from a sample of 50 g urea which contains 47% nitrogen and from wheat-flour. Fig. 2 shows details around the three peaks related to the 10.8 MeV radiation. In the figure is also plotted a

spectrum for a sample of glucose containing the same percentage of hydrogen as urea. As the figure shows this sample gave no detectable contribution to the background in the 10 MeV region, indicating that the effect of the neutron scattering is negligible.

The results of these preliminary experiments show that the method will be well suited for the purpose in question.

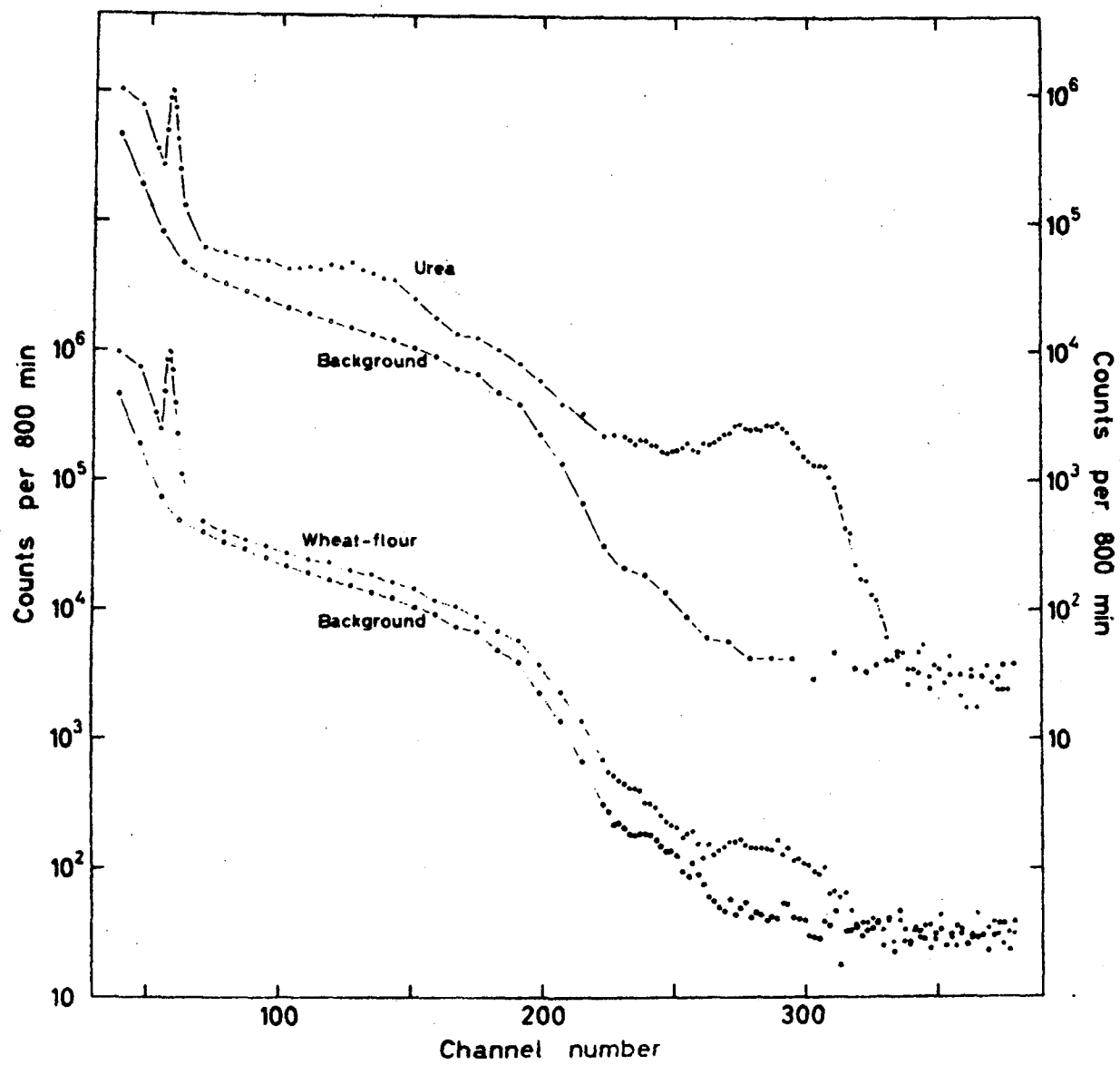


Fig. 1.

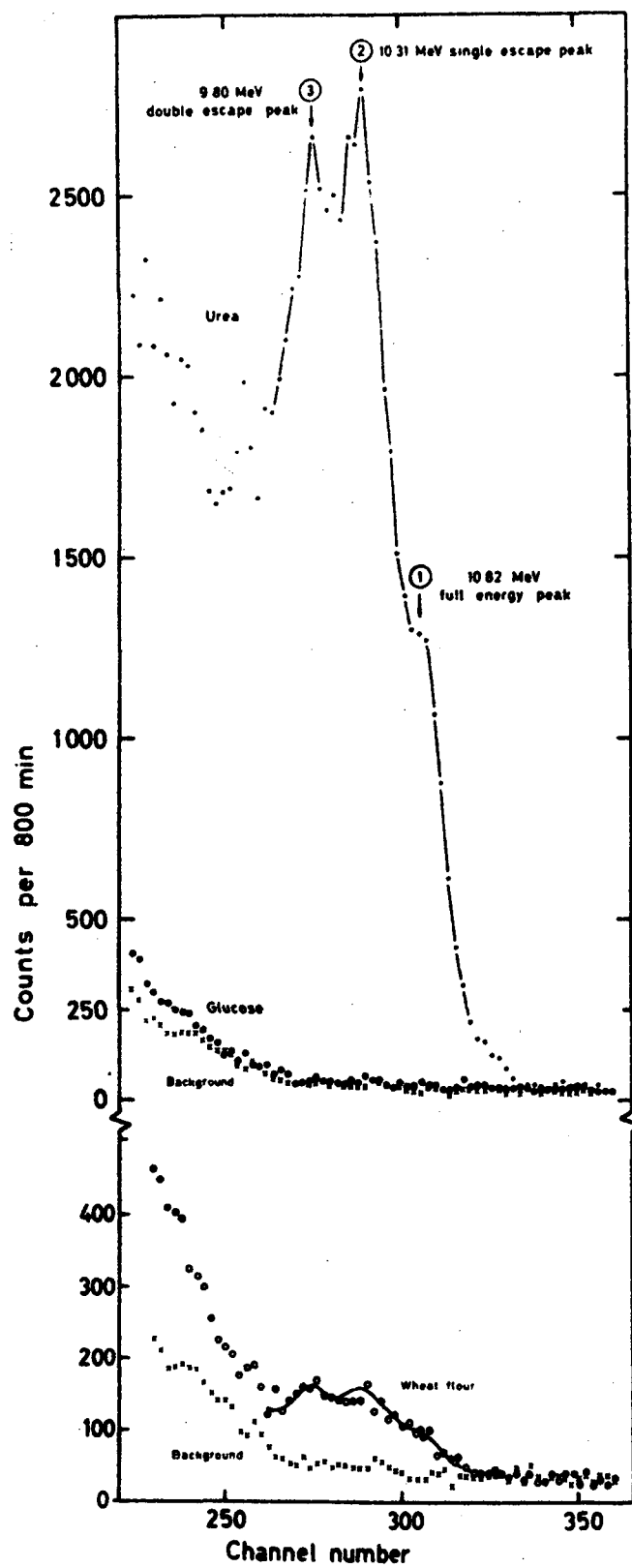


Fig. 2

2. General Neutron Physics

2.1 Studies of (d,py) reactions in nuclei with mass numbers around $A = 50$

I. Bergqvist and L. Carlén
Department of Physics, University of Lund, Lund
Sweden
L. Nilsson
Tandem Accelerator Laboratory, Uppsala, Sweden

These experiments, which have been described in the preceding EANDC report, have two main purposes. They aim at an understanding of the neutron capture mechanism in nuclei in the $A = 50$ mass region. They are also designed to give spectroscopic information on bound levels in the residual nuclei.

Gamma radiation in coincidence with protons has previously been detected by a large NaI(Tl) scintillator. To obtain better energy resolution and thus to improve the spectroscopic information, a two-parameter arrangement using a Ge(Li) detector and a surface barrier detector has been tested at the Tandem Accelerator Laboratory. A recent experiment with an isotopically enriched ^{56}Fe target seems to be very promising for future experiments of this kind.

3. Theoretical Physics

3.1 Shell model calculations of level densities

J. Eriksson
Neutron Physics Laboratory, Studsvik, Nyköping,
Sweden

Estimates of reaction cross sections by model calculations often involve the knowledge of excited nuclear levels as functions of energy, spin and parity. The most often used parametrization for this purpose is obtained from the assumption of an enclosed Fermi gas. This type of level density increases smoothly with the excitation energy. In applications, states in the region of the first few MeV excitation are of particular interest. However, experimentally determined level-distributions for non-rare nuclei for these energies develop strong fluctuations essentially due to the effect of the shell structure. The applied model of exact counting of shell model states is the most promising way to improve upon the theoretical predictions of nuclear level densities.

A very simple system of six nucleons sitting in five doubly degenerate single particle levels is shown in Fig. 1. The nucleus may exist in eigenstates of the standard pairing Hamiltonian with a pairing force constant here equal to the level spacing. As seen from Fig. 1 our interpolative technique of solving the pairing Hamiltonian compares well with the set of exact solutions for seniorities 0, 2 and 4. Fig. 2 shows the resulting level-density of the nucleus ^{58}Ni for realistic single particle level schemes and pairing of protons and neutrons. In this calculation there are totally 31 single particle levels taken into account.

As can be seen the important parity of levels is also obtained through the exact counting of shell levels.

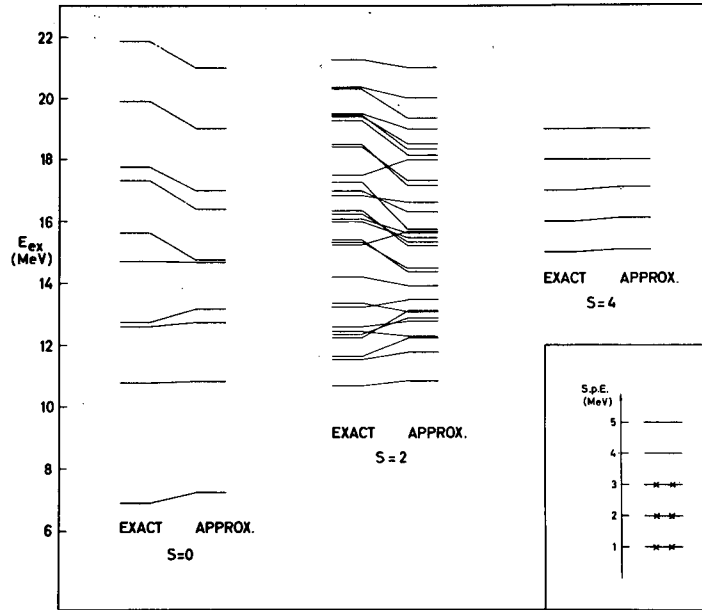


Fig. 1 A simple case of exact counting excited states for a system of six nucleons occupying five spin $\frac{1}{2}$ levels. Seniority 0, 2 and 4 states are shown for the exact results and for our interpolative approximations.

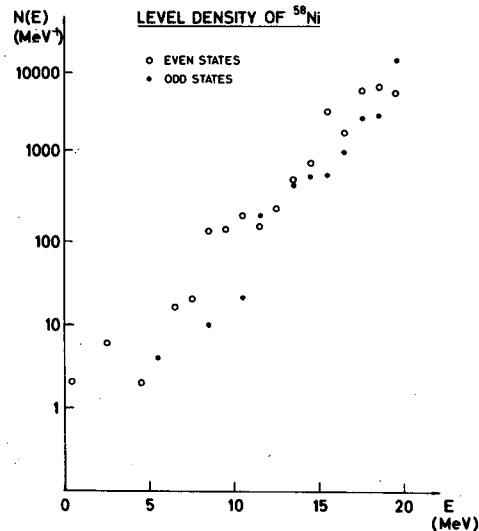


Fig. 2 The level density of ^{58}Ni calculated from realistic neutron and proton single particle level schemes.

3.2 Calculation of semidirect nucleon radiative capture cross sections including spin-orbit and interference effects

J. Eriksson
Neutron Physics Laboratory, Studsvik, Nyköping,
Sweden

The radiative capture cross section of neutrons shows a pronounced broad peak in the region of about 8-15 MeV. The simple model of a direct neutron capture process does not develop this picture but rather leads to results an order of magnitude below the experimental cross sections. To rectify this a semidirect (or collective) model was introduced independently by Brown [1] and by Clement et al. [2] some years ago. Both models propose that the captured neutron excites the target nucleus into its giant-dipole state. Upon deexcitation of the giant-dipole state a photon may be emitted. The theories as given [1,2] did not include the spin algebra which for this reason was considered in an earlier work [3]. However the spin-completed calculations still gave up to two times too small (n,γ) -cross sections. This led to the proposal that direct capture by interference might help to reduce the remaining discrepancy. This has in yet unpublished calculations turned out to be partly true. Thus at this stage of adding direct and semidirect amplitudes the semidirect capture theory is essentially able to explain experimental data. Efforts to take care of the remaining discrepancy by varying the surface concentrated formfactor of the neutron to giant resonance coupling were not successful. It thus appears that for instance the compound nuclear mechanism [4] may contribute significantly.

- [1] G.E. Brown, Nucl. Phys. 57 (1964) 339.
- [2] C.F. Clement, A.M. Lane and J.R. Rook, Nucl. Phys. 66 (1965) 273, 293
- [3] J. Eriksson, FN-TPM-2 (1971) AE internal report
- [4] D. Sperber, Phys. Rev. 184 (1969) 1201

4. Van de Graaff-accelerator, Studsvik

4.1 Accelerator Performance

P. Tykesson and B. Jonsson

The Van de Graaff accelerator has been run with protons, deuterons and helium ions, with both DC beams and pulsed beams. The accelerator was run in two and three shifts for 5 days per week and the calculated total time available for experiments was 3093 hours: of these 2940 hours were used by scientists, 80.5 hours were used for machine tests and 72.5 hours were required for unforeseen maintenance.

The distribution of the available machine time between experiments performed by physicists from various institutes is shown in Table 1, and between different experimental branches in Table 2.

Table 1

The distribution of the machine time between various institutes

AB Atomenergi	67.7
Research Institute of National Defence (FOA)	17.6
University of Lund	5.3
Chalmers University of Technology	5.2
University of Aarhus, Denmark	4.2

Table 2

The distribution of the machine time between different experimental branches

Neutron physics	50.5
Nuclear physics	20.2
Solid state physics	13.8
Materials physics	11.1
Machine tests	2.7
Irradiations	1.7

There were three normal breaks for maintenance of the machine during the period: two of these lasted for one week, while the break connected with the change of the accelerator tube lasted about two months.

4.2 Crossed field analyser

P. Tykesson and B. Jonsson

The crossed field analyser was used in the machine for ${}^3\text{He}^{++}$ and high-proton-current runs, for a total of about 459 hours during the period. However, the lifetime of the ion sources was short (50 hours) during ${}^3\text{He}^{++}$ -runs, owing to trouble with contamination on the quartz bushing around the source canal. Two types of canal were tested, namely a stainless steel-lined aluminium canal and a nickel canal, but the tests revealed no difference in lifetime. Tantalum-lined aluminium canals will be tested in the near future.

4.3 Installation of a solid state power supply

P. Tykesson and B. Jonsson

While the accelerator tube was being exchanged, a new solid state power supply ^{x)} for the analysing magnet was installed. The new power supply replaces the 11-year-old motor-generator set which was delivered at the same time as the accelerator. The reason for replacing the old power supply was that some new experiments demand an increased stability, beyond that which could be achieved with the old power supply. The newly installed equipment has made a considerable contribution to the increased stability and reliability.

x) Type PS3.6-60 made by Scanditronix AB

4.4 Change of accelerator tube

P. Tykesson and B. Jonsson

The accelerator tube was installed in 1960 and has been in operation for approximately 29.500 hours. During the 1970's, however, it has not been possible to operate the machine at maximum voltage. This was due to a worn-out accelerator tube and inherent changes of the resistors in the voltage divider. Just before the machine was shut down it was run at a voltage of 4.5 MV and with five sections of the tube shortened. After the accelerator tube had been dismantled it was found necessary to shorten an additional six sections. It was also found that the insulations between the accelerator tube electrodes at the beginning of the tube were damaged. The values of the resistors deviated from the original ones: in almost all cases it was found that they had increased. During the break for the changing the accelerator tube, the column was completely dismantled. This was cleaned and inspected, and the new column resistors from HVEC were mounted. The belt of the accelerator was also found to be in a rather poor state, and it was therefore decided that this should be replaced by a new one. In order to decrease the electron loading in the accelerator tube, electric fields were applied at the far end of the tube so as to inhibit electrons passing in the opposite direction to the protons. The mounting of the column and the accelerator tube took approximately one month. This was followed by a three-week period during which the accelerator tube and the terminal were conditioned up to a voltage of 4.5 MV.

The performance and reliability of the machine have improved considerably during the last year. This is mainly a result of the installation of a new accelerator tube and new column resistors. The new solid state power supply for the analyzing magnet has helped to improve the energy resolution and consequently also the overall performance of the experimental facilities.

5. Tandem Accelerator Laboratory, Uppsala

5.1 The neutron time-of-flight facility at the Uppsala Tandem Accelerator

H. Condé, C. Nordborg, L-E. Persson and
L.G. Strömberg
The Research Institute of the Swedish National
Defence, Stockholm, Sweden

A. Lindholm and G. Lodin
Department of Physics, University of Uppsala,
Uppsala, Sweden

L. Nilsson
Tandem Accelerator Laboratory, Uppsala, Sweden

Neutron-induced reactions

The pulsed ion source at the tandem accelerator is capable of producing short beam bursts of various ions at frequencies in the Mhz region. This offers a good opportunity to study neutron-induced reactions. Mono-energetic neutrons in the MeV region are produced with gas targets using reactions such as ${}^3\text{H}(p,n){}^3\text{He}$ and ${}^2\text{H}(d,n){}^3\text{He}$. The detector arm, capable of holding heavy shieldings is designed to satisfy demands from various types of nuclear physics experiments involving neutrons. Until now only calibrations and efficiency measurements have been performed, but future plans are to study neutron capture in the giant resonance region and $(n,n'\gamma)$ processes in light nuclei, and if possible also (n,f) and $(n,2n)$ reactions.

(Charged particle,n) reactions

Experiments where neutron spectra from (charged particle,n) reactions are studied put heavy demands on the time-of-flight facility. To achieve optimum neutron-energy resolution and reasonable intensities the accelerator must deliver short beam bursts at high

average ion currents, the detector must give fast response and have high efficiency and the movable detector arm must allow for long flight paths within a large angular range. Preliminary measurements on (d,n) reactions in nuclei with mass-numbers between 50 and 60 have been started. We are also planning to perform in the near future ($^3\text{He},n$) experiments and coincidence measurements on (charged particle, $n\gamma$) reactions.